

University of Groningen

## The relevance of the non-canonical PTS1 of peroxisomal catalase

Williams, Chris; Aksam, Eda Bener; Gunkel, Katja; Veenhuis, Marten; van der Klei, Ida J.

*Published in:*  
Biochimica et Biophysica Acta-Molecular Cell Research

*DOI:*  
[10.1016/j.bbamcr.2012.04.006](https://doi.org/10.1016/j.bbamcr.2012.04.006)

**IMPORTANT NOTE: You are advised to consult the publisher's version (publisher's PDF) if you wish to cite from it. Please check the document version below.**

*Document Version*  
Publisher's PDF, also known as Version of record

*Publication date:*  
2012

[Link to publication in University of Groningen/UMCG research database](#)

*Citation for published version (APA):*

Williams, C., Aksam, E. B., Gunkel, K., Veenhuis, M., & van der Klei, I. J. (2012). The relevance of the non-canonical PTS1 of peroxisomal catalase. *Biochimica et Biophysica Acta-Molecular Cell Research*, 1823(7), 1133-1141. <https://doi.org/10.1016/j.bbamcr.2012.04.006>

### Copyright

Other than for strictly personal use, it is not permitted to download or to forward/distribute the text or part of it without the consent of the author(s) and/or copyright holder(s), unless the work is under an open content license (like Creative Commons).

The publication may also be distributed here under the terms of Article 25fa of the Dutch Copyright Act, indicated by the "Taverne" license. More information can be found on the University of Groningen website: <https://www.rug.nl/library/open-access/self-archiving-pure/taverne-amendment>.

### Take-down policy

If you believe that this document breaches copyright please contact us providing details, and we will remove access to the work immediately and investigate your claim.

*Downloaded from the University of Groningen/UMCG research database (Pure): <http://www.rug.nl/research/portal>. For technical reasons the number of authors shown on this cover page is limited to 10 maximum.*



## The relevance of the non-canonical PTS1 of peroxisomal catalase

Chris Williams<sup>b,1</sup>, Eda Bener Aksam<sup>a,1</sup>, Katja Gunkel<sup>a</sup>, Marten Veenhuis<sup>a</sup>, Ida J. van der Klei<sup>a,\*</sup>

<sup>a</sup> Molecular Cell Biology, Groningen Biomolecular Sciences and Biotechnology Institute, Kluyver Centre for Genomics of Industrial Fermentation, University of Groningen, P.O. Box 11103, 9700 CC Groningen, The Netherlands

<sup>b</sup> European Molecular Biology Laboratory, Structural Biology Unit, Notkestrasse 85, 22603, Hamburg, Germany

### ARTICLE INFO

#### Article history:

Received 29 January 2012  
Received in revised form 12 April 2012  
Accepted 16 April 2012  
Available online 21 April 2012

#### Keywords:

Catalase  
Peroxisome  
Yeast  
Protein sorting  
Protein assembly

### ABSTRACT

Catalase is sorted to peroxisomes via a C-terminal peroxisomal targeting signal 1 (PTS1), which binds to the receptor protein Pex5. Analysis of the C-terminal sequences of peroxisomal catalases from various species indicated that catalase never contains the typical C-terminal PTS1 tripeptide-SKL, but invariably is sorted to peroxisomes via a non-canonical sorting sequence. We analyzed the relevance of the non-canonical PTS1 of catalase of the yeast *Hansenula polymorpha* (-SKI). Using isothermal titration microcalorimetry, we show that the affinity of *H. polymorpha* Pex5 for a peptide containing -SKI at the C-terminus is 8-fold lower relative to a peptide that has a C-terminal -SKL. Fluorescence microscopy indicated that green fluorescent protein containing the -SKI tripeptide (GFP-SKI) has a prolonged residence time in the cytosol compared to GFP containing -SKL. Replacing the -SKI sequence of catalase into -SKL resulted in reduced levels of enzymatically active catalase in whole cell lysates together with the occurrence of catalase protein aggregates in the peroxisomal matrix. Moreover, the cultures showed a reduced growth yield in methanol-limited chemostats. Finally, we show that a mutant catalase variant that is unable to properly fold mislocalizes in protein aggregates in the cytosol. However, by replacing the PTS1 into -SKL the mutant variant accumulates in protein aggregates inside peroxisomes. Based on our findings we propose that the relatively weak PTS1 of catalase is important to allow proper folding of the enzyme prior to import into peroxisomes, thereby preventing the accumulation of catalase protein aggregates in the organelle matrix.

© 2012 Elsevier B.V. All rights reserved.

### 1. Introduction

Catalase is an important antioxidant enzyme that decomposes hydrogen peroxide into water and oxygen. The active enzyme is a homo-tetrameric protein of approximately 240 kDa, which contains 4 heme molecules [1].

In most eukaryotes catalase is confined to peroxisomes. Peroxisomes are subcellular organelles that occur in all eukaryotes and are involved in a large variety of processes, which depend on species, cell type and developmental stage. By definition, they contain catalase in conjunction with at least one hydrogen peroxide producing oxidase. The presence of catalase at the site of hydrogen peroxide production is assumed to prevent the leakage of this reactive compound from the organelle to other cellular compartments [2].

Mammals invariably contain a single catalase gene, which encodes a peroxisomal enzyme. The same is true for most yeast species. An exception however is *Saccharomyces cerevisiae*, which has two catalase genes, encoding cytosolic (catalase T) and peroxisomal catalase (catalase A) [3]. Plants generally contain three catalase genes, which all encode peroxisomal enzymes [4,5].

Sorting of peroxisomal catalases depends on Pex5, the peroxisomal targeting signal 1 (PTS1-) receptor. The canonical PTS1 sequence is the tripeptide (S/A/C)(K/R/H)(L/M) at the extreme C-terminus. These conserved tripeptides are generally present in high-abundant peroxisomal matrix proteins. In addition, peroxisomal matrix proteins exist that have non-canonical C-terminal tripeptides. These are much less conserved and generally occur on low abundant peroxisomal matrix proteins. Where the canonical PTS1 sequence is generally sufficient to target a reporter to peroxisomes, non-canonical PTS1 sequences often require auxiliary targeting information [6–10]. Based on detailed studies on the interaction of the PTS1 binding domain of Pex5 with various proteins/peptides, the PTS1 is now defined as a C-terminal 12 amino acid sequence, which consists of the C-terminal tripeptide that interacts with the PTS1-binding site in Pex5, a tetrapeptide immediately upstream this tripeptide, which may interact with the surface of Pex5, and a flexible hinge of 5 residues (reviewed in [8]).

Peroxisomal catalase, although being a conserved and relatively abundant protein, does not have a canonical PTS1 sequence in any of the organisms studied so far (see Table 1). For instance, peroxisomal catalases of the methylotrophic yeast species *Candida boidinii* and *Hansenula polymorpha* contain the C-terminal tripeptides -NKF and -SKI respectively [11,12]. Also, catalases may have very unusual PTS1 variants, such as the tetrapeptide -KANL of human catalase [13] and

\* Corresponding author. Tel.: +31 50 363 2179; fax: +31 50 363 2400.  
E-mail address: [i.j.van.der.klei@rug.nl](mailto:i.j.van.der.klei@rug.nl) (I.J. van der Klei).

<sup>1</sup> These authors equally contributed to the work.

**Table 1**  
C-terminal sequences of peroxisomal catalases.

Organism	Protein name	C-terminus	Reference
<i>Cucurbita pepo</i>	cat1	KLASHLNVRPSI	[48]
<i>Cucurbita pepo</i>	cat2	KIASRMNARPNM	[48]
<i>Cucurbita pepo</i>	cat3	KIASRLNVRPNI	[48]
<i>Gossypium hirsutum</i>	Ccat	KIASRLNVRPSI	[5]
<i>Aspergillus nidulans</i>	catC	TEKKATEARARL	[49]
<i>Caenorhabditis elegans</i>	cat-2	KALIQKQARSHI	[50]
<i>Candida boidinii</i>	Cta1	KKSPRGASKNKF	[11]
<i>Hansenula polymorpha</i>	Cat	ELKRKASSPSKI	[12]
<i>Saccharomyces cerevisiae</i>	CatA	KHASELSSNSKF	[14]
<i>Homo sapiens</i>	Cat	GSHLAAREKANL	[13]
<i>Rattus norvegicus</i>	Rcat	GSHIAAKGKANL	[51]
<i>Mus musculus</i>	Mcat	GSHMAAKGKANL	[51]
<i>Bos taurus</i>	Bcat	GSHLSAREKANL	[52]

the hexapeptide -SSNSKF in *S. cerevisiae* catalase A [14]. Moreover, the C-terminal PTS in *S. cerevisiae* catalase A was reported to be redundant for sorting, as the protein contains a second, internal peroxisomal sorting signal, present between residues 104 and 126 [14]. Although largely conserved between *S. cerevisiae* and *H. polymorpha* catalase (for an alignment see [15]), the role of this region in Pex5p binding is unknown, as it is not surface exposed [16]. Pumpkin Cat1 also contains an internal peroxisomal sorting signal, near its C-terminus, in addition to a redundant PTS1 sequence at the extreme C-terminus [17]. The role of this region, which appears to be conserved in plants but not in other catalase proteins, in Pex5p binding remains to be determined.

In vitro binding studies, using the PTS1 binding domain of human Pex5, indicated that peptides containing the typical PTS1 sequence -SKL have a higher affinity for Pex5 compared to the other PTS1 variants that were tested [18–20]. This poses the question of the significance of the unusual PTS1 sorting signals of catalase.

Here we analyzed the non-canonical PTS1 of *H. polymorpha* catalase. First, we show that this sequence is required for import of the protein into peroxisomes. In vitro studies revealed that *H. polymorpha* Pex5p has an eightfold lower affinity for the -SKI tripeptide of catalase relative to the typical -SKL sequence. Replacing the -SKI sequence by the stronger -SKL sequence resulted in import of the protein into peroxisomes, but also in a decrease in catalase enzyme activities in conjunction with the formation of catalase protein aggregates in the organelle matrix. Hence, our results suggest that the non-canonical, weak PTS1 of *H. polymorpha* catalase contributes to obtaining high levels of enzymatically active catalase inside peroxisomes in vivo.

## 2. Materials and methods

### 2.1. Organisms and growth

The *H. polymorpha* strains used in this study are listed in Table 2. *H. polymorpha* cells were grown in batch cultures at 37 °C on selective YND media containing 0.67% yeast nitrogen base without amino acids or mineral media (MM). Media were supplemented with 0.5% glucose or 0.5% methanol as carbon source and 0.25% ammonium sulfate as nitrogen source. When required, amino acids or uracil was added to a final concentration of 30 µg/ml.

Cells were grown in methanol-limited chemostat cultures (dilution rate 0.07 h<sup>-1</sup>) at a pH of 5.0. The feed contained 0.4% (v/v) methanol and 60 µg/ml leucine.

For growth on agar plates the media were supplemented with 2% agar. For selection of resistant transformants, YPD plates containing 100 µg/ml zeocin (Invitrogen, Breda, The Netherlands) were used.

For cloning purposes *Escherichia coli* DH5α was used. Cells were grown at 37 °C in LB supplemented with 100 µg/ml ampicillin or kanamycin when required.

**Table 2**  
*H. polymorpha* strains used in this study.

Strain	Properties	Reference
Wild type <i>leu1.1</i>	NCYC495 <i>leu1.1</i>	[53]
cat-SKI	Strain containing wild-type CAT-SKI, <i>leu1.1</i> , <i>Zeo</i> <sup>R</sup>	This study
cat-SKL	Endogenous CAT-SKI replaced by CAT-SKL, <i>leu1.1</i> , <i>Zeo</i> <sup>R</sup>	This study
<i>cat::URA3</i>	Catalase deletion strain, <i>leu1.1</i>	[54]
Cat-Y348G	Strain containing point mutation in heme binding site of catalase	This study
Cat-Y348G-SKL	Strain containing point mutation in heme binding site of catalase, together with replacement of -SKI by -SKL	This study
Cat-SKI	Strain producing Cat-SKI	This study
Cat-SKK	Strain producing Cat-SKK	This study
WT::P <sub>AOX</sub> GFP-SKL	Wild-type producing eGFP-SKL under control of the alcohol oxidase promoter <i>leu1.1</i> <i>Zeo</i> <sup>R</sup>	[35]
WT::P <sub>AOX</sub> GFP-SKI	Wild-type producing eGFP-SKI under control of the alcohol oxidase promoter, <i>leu1.1</i> <i>Zeo</i> <sup>R</sup>	[34]

Full length *H. polymorpha* Pex5p was produced in the *E. coli* strain BL21 DE3 (B, F-, dcm, ompT, hsdS (rB<sup>-</sup> mB<sup>-</sup>), gal λ(DE3)). Cells were grown at 37 °C to an OD<sub>600</sub> of 0.4 in LB medium supplemented with antibiotics, transferred to 21 °C and grown further until an OD<sub>600</sub> of 0.7. Protein production was then induced with 1 mM IPTG (Invitrogen) for 4 h.

### 2.2. Peptides

The peptides YELKRKASSPSKI and YELKRKASSPSKL were synthesized by Pepscan (Lelystad, The Netherlands). The purchased peptides were HPLC purified and quality was assessed with LC/MS. The concentrations of peptides were estimated using a Nanodrop™ ([www.nanodrop.com](http://www.nanodrop.com)).

### 2.3. Molecular techniques

Plasmids and primers used in this study are listed in Tables 3 and 4. Standard recombinant DNA techniques were carried out essentially as described before [21]. Transformation of *H. polymorpha* cells and site specific integration in the *H. polymorpha* genome were performed as described previously. DNA modifying enzymes were used as recommended by the suppliers (Roche, Almere, The Netherlands and Fermentas, St. Leon-Rot, Germany). *Pwo* polymerase was used for preparative polymerase chain reactions (PCR). Oligonucleotides were synthesized by Biogio (Nijmegen, The Netherlands). DNA sequencing reactions were performed at Service XS (Leiden, The Netherlands). For DNA sequence analysis, the Clone Manager 5 program (Scientific and Educational Software, Durham, USA) was used. BLAST algorithms were used to screen databases at the National Center for Biotechnology Information (Bethesda, MD).

### 2.4. Construction of the Cat-SKL strain

The endogenous PTS1 of catalase (-SKI) was replaced by -SKL by changing the ATA codon into a CAG codon by double recombination. Plasmid pEBA0029 containing the double recombination cassette was created as follows. Cat-SKL PCR fragment I, which contained the code for the SKL sequence, was obtained by using the primers “BJ clo1 fw” and “BJ clo1 rev” (Table 4) and *H. polymorpha* wild-type genomic DNA as a template. This fragment and the pBS-zeo plasmid containing the zeocin marker were digested with *Sac*II and *Xba*I and ligated, resulting in plasmid pEBA0028. The PCR fragment II, which corresponds to the 3' end flanking region of the catalase gene, was amplified by using the primers “BJ clo2 fw” and “BJ clo2 rev” and

**Table 3**  
Plasmids used in this study.

Plasmid	Relevant properties	Reference
pBS-zeo	pBluescript II KS <sup>+</sup> containing the zeocin selection cassette	[55]
pEBA0028	pBS-zeo containing the 3' end of the CAT gene with I507L (SKI→SKL) mutation.	This study
pEBA0029	pBS-zeo containing the CAT-SKL double recombination cassette	This study
pCW220	His <sub>6</sub> -GST HpPex5p for synthesis in <i>E. coli</i>	This study
pAKR0043	pBS-zeo containing the CAT-SKI double recombination cassette	This study
pB-CAT-DN	pBluescript SK <sup>+</sup> containing CAT Y348G	This study
pBluescript II SK <sup>+</sup>	<i>E. coli</i> plasmid	Stratagene, La Jolla, CA
pGEM-5Zf(+)	pGEM@-T Easy Vector System I	Promega Corporation, Madison, WI, USA
pHIPX9-Cat-Y348G	pHIPX9 containing CAT Y348G under control of P <sub>CAT</sub>	This study
pHIPX9-Cat-Y348G.SKL	pHIPX9 containing CAT Y348G under control of P <sub>CAT</sub> and the PTS1 -SKL at the C-terminus	This study
pHIPX9-Cat.SKI	pHIPX9 containing CAT under control of P <sub>CAT</sub>	This study
pHIPX9-Cat.SKK	pHIPX9 containing CAT encoding catalase with C-terminal -SKK under control of P <sub>CAT</sub>	This study
pHIPX9	Shuttle vector containing P <sub>CAT</sub>	Lab collection
pHCAT-B	Shuttle vector containing CAT	[12]
pHCAT-K	Shuttle vector containing CAT gene encoding catalase with C-terminal -SKK	[12]

wild-type genomic DNA as a template. Subsequently, this fragment and plasmid pEBA0028 were digested with *Acc65I* and *XhoI* and ligated to produce pEBA0029. Plasmid pEBA0029 was digested with *SacII* and *Acc65I*. The resulting 2715 base pair fragment containing the CAT-SKL gene was transformed to wild-type *H. polymorpha* cells. Replacement of the wild-type CAT gene by the CAT-SKL gene in the genome at the correct position was confirmed by Southern blot analysis.

### 2.5. Construction of the Cat-SKI strain

For the construction of plasmid pAKR0043, a PCR fragment of 801 bp was obtained by primers AKR0027cat1fwd and AKR0028cat1rev using plasmid pEBA0029 as a template. This PCR fragment and plasmid pEBA0029 were digested with *XbaI* and *SacI* and ligated to produce

**Table 4**  
Primers used in this study.

Name	Sequence
Bj clo 1 fwd	ACGACTAACCCGGGAGACTTGTGGGAAGCAATTGAGAA
Bj clo 1 rev	ACGTTCTATTCTAGATTACAGTTTGGATGGAGAAGAAGCC
Bj clo 2 fwd	TCAACAACCTCCCTCGAGTATTATAGCTTCCTGATCTGG
Bj clo 2 rev	CTGTCTGTATGGTACCTTCATGGCAGTCTTGAGATCGTAG
HpP5 (F)	GCCATGGCAITTTCTGGGAGGATCGG
HpP5 (R)	GGAAGCTTTTATATGCTGAGGTTTTTCGGAACGA
CAT-UP-Prom	CGACGGTGTAACACGCTGCAGCTCGC
CAT-DN	CTGTATGATTTGAGCACATCCGGACAAGC
CAT-C-term-DN	GGATGATACGGCGGACAGGAC
CAT-SKL-SalI-DN	TACATCGTCGACGATTAAGTTTGGATGGAGAAGAAGCC
CAT-ApaI Y348G-DN	CTGTGTCTGTGCTGTCTGGGCCGAAAACAGTCTCGATTGC
CAT-ApaI Y348G-UP	GCAATCGAGACTGTTTTCCGGCCAGACACGACACAGACAG
AKR0027cat1fwd	ATTGGAGCTCCACCGGGGAGACTTGTGGGA
AKR0028cat1rev	CAGCTATGACTCTAGATTATATTTGGATGG

pAKR0043. Correct plasmid construction was confirmed by sequence analysis. The plasmid pAKR0043 was digested with *PvuI*, *Cfr42I* and *Acc65I* and the 2715 base pair fragment containing the CAT-SKI gene was transformed to wild-type *H. polymorpha* cells. Zeocin resistant colonies were checked with PCR. Correct integration was confirmed by Southern blot analysis.

### 2.6. Construction of a point mutation in the heme binding site

To create catalase mutants disturbed in binding the heme cofactor, the conserved tyrosine Y348 which serves as heme proximal side ligand (see Accession no.: P30263) was changed into glycine. First, the catalase gene was amplified by PCR, thereby changing T into G at nucleotide position 1044, resulting in the formation of an *Apal* restriction site. The downstream region of the catalase gene was amplified using primers CAT-*Apal* Y348G-UP and CAT-DN (Table 4); the resulting fragment of 943 bp was digested with *Apal* and inserted in pBluescript II SK<sup>+</sup> digested with *Apal* and *NaeI*. The resulting plasmid was designated pB-CAT-DN. Upon digestion of pB-CAT-DN with *Apal* and *EcoRV*, a 623 bp fragment (Y348G-Cat-DN) was obtained. The upstream region of the catalase gene, with a size of 1706 bp, was amplified using primers CAT-UP-Prom and CAT-*Apal* Y348G-DN (Table 2). The obtained fragment was cloned in pGEM-5Zf(+). Subsequently, the plasmid was digested with *SphI* and *Apal*, resulting in a fragment (Y348G-Cat-UP) of approximately 1.1 kbp. Vector pHIPX9 was digested with *SphI* and *SmaI* and ligated with the two fragments Y348G-Cat-UP and Y348G-Cat-DN. The resulting plasmid, pHIPX9-Cat-Y348G, was digested with *SphI* for directed integration in the catalase promoter region in *H. polymorpha* NCYC 495 *cat* (*leu1.1*). Correct integration was confirmed by Southern blotting. The resulting strain was designated Cat-Y348G.

Plasmid pHIPX9-Cat-Y348G was also used as a template to construct plasmid pHIPX9-Cat-Y348G.SKL, encoding catalase containing a point mutation in the heme binding site and an -SKL at the extreme C-terminus, instead of -SKI. To this purpose the catalase gene was amplified using primers CAT-UP-Prom and CAT-SKL-SalI-DN. Vector pHIPX9 was digested with *SphI* and *SalI* and ligated with the 1.6 kbp PCR-fragment digested with the same enzymes. The resulting pHIPX9-Cat-Y348G.SKL was linearized with *SphI* and integrated in the catalase promoter of *H. polymorpha* NCYC 495 *cat* (*leu1.1*). Correct integration was analyzed by Southern blotting. The constructed strain was designated Cat-Y348G.SKL.

### 2.7. Construction of a strain producing catalase with -SKK at the extreme C-terminus

To construct genes, encoding the catalase with -SKI or the modified C-terminal tripeptide -SKK, plasmids pHCAT-K and pHCAT-B were used as template for amplification of the catalase genes with primers CAT-UP-Prom and CAT-C-term-DN. Fragments of 2.3 kbp were digested with *SphI* and integrated in pHIPX9, digested with *SphI* and *SmaI*. The resulting plasmids pHIPX9-Cat.SKI and pHIPX9-Cat.SKK were linearized with *SphI* and integrated in the catalase promoter region of NCYC 495 *cat* (*leu1.1*). Correct integration was analyzed by Southern Blot analysis. The resulting strains were designated Cat.SKI and Cat.SKK, respectively.

### 2.8. Construction of the His<sub>6</sub>-GST Pex5 expression plasmid

To construct plasmid pCW220, the His<sub>6</sub>-GST Pex5p expression plasmid, PCR was performed on genomic DNA using primers HpP5(F) and HpP5(R). The resulting product was digested with *NcoI* and *HindIII* and ligated into *NcoI*-*HindIII* digested pETM30.

## 2.9. Biochemical methods

Crude extracts of *H. polymorpha* cells were prepared as described previously [22]. Catalase activity was measured according to Lück (1963) [23]. Protein concentrations were determined using the Biorad Protein Assay system (Biorad GmbH, Munich, Germany) using bovine serum albumin as a standard. Sodium dodecyl sulfate-polyacrylamide gel electrophoresis (SDS-PAGE) [24] and Western blotting [25] were performed as described before.

## 2.10. Purification of full length *H. polymorpha* Pex5p

Cell pellets were thawed in lysis buffer (50 mM Tris, pH 7.5, 150 mM NaCl, 1 M urea, 5% ethanol, 3 mM  $\beta$ -mercaptoethanol, 2 mM PMSF), treated with 1 mg/ml lysozyme and then pulse sonicated on ice. Cell debris was removed by centrifugation and lysates were loaded onto glutathione sepharose-4B resin (GE Healthcare) pre-equilibrated with lysis buffer. The resin was sequentially washed with lysis buffer, buffer W1 (50 mM Tris, pH 7.5, 1 M NaCl, 3 mM  $\beta$ -mercaptoethanol) and buffer W2 (50 mM Tris, pH 7.5, 150 mM NaCl, 2 mM  $\beta$ -mercaptoethanol) and His<sub>6</sub>-GST Pex5p was eluted with buffer W2 containing 20 mM reduced glutathione. The His<sub>6</sub>-GST tag was removed by cleavage with His<sub>6</sub>-TEV and the sample was applied to Ni-NTA agarose (Qiagen), to remove the GST tag, TEV and undigested fusion protein. Pex5p was further purified by gel filtration on a Superdex 200 (16/60) column (GE Healthcare). Purity was monitored by SDS-PAGE analysis and protein concentration was estimated using a Nanodrop™ ([www.nanodrop.com](http://www.nanodrop.com)).

## 2.11. Fluorescence- and electron microscopy

Fluorescence microscopy was performed on a Zeiss Axioskop50 fluorescence microscope. Images were taken with a Princeton Instruments 1300Y digital camera. GFP signal was visualized with a 470/40-nm bandpass excitation filter, a 495-nm dichromatic mirror, and a 525/50-nm bandpass emission filter. All GFP images were processed with the same settings in the program Adobe Photoshop cs2.

Whole cells were fixed and prepared for electron microscopy and immunocytochemistry as described before [26]. Immunolabeling was performed on ultrathin sections of Unicryl-embedded cells, using specific polyclonal antiserum against catalase and gold-conjugated goat-anti-rabbit antiserum [26].

## 2.12. Isothermal titration microcalorimetry (ITC) measurements

Prior to ITC measurements, proteins and peptides were dialyzed against 25 mM Tris pH 7.5, 150 mM NaCl, 2 mM  $\beta$ -Mercaptoethanol. Measurements with Pex5p (28–35  $\mu$ M) as a sample and peptide (280–350  $\mu$ M) as the titration ligand were performed at 25 °C, using a MicroCal VP-ITC and data were fitted with MicroCal Origin 7.0. Values measured during titrations are presented in Table 5 and correspond to the dissociation constant (K<sub>d</sub>), the reaction stoichiometry (n), the changes in enthalpy ( $\Delta$ H) and entropy ( $\Delta$ S). The Gibbs free energy ( $\Delta$ G) is calculated according to the equation  $\Delta G = \Delta H - T\Delta S$ , where T is the temperature.

## 2.13. Modeling of the SKI–Pex5p interaction

A model of the cargo binding region of *H. polymorpha* Pex5p was constructed using SWISS-MODEL (<http://swissmodel.expasy.org/>) with Pex5p from the Pex5p–SCP2 structure (PDB code 2C0L, [27]) as template. This model, consisting of residues 259–568, was aligned against the eight available Pex5p–cargo structures from the human (PDB codes 1FCH, 2C0L and 3R9A) and trypanosome (PDB codes 3CV0, 3CVL, 3CVN, 3CVP and 3CVQ) proteins. An additional model, based on the Pex5p–YQSKL structure (PDB code 1FCH, [28]) but

containing an Ile, rather than Leu at the –1 position (constructed with the molecular graphics program COOT [29]), was also included in the alignment.

## 3. Results

### 3.1. The C-terminal tripeptide -SKI is required for catalase sorting

We first analyzed whether the C-terminal -SKI sequence of *H. polymorpha* catalase is required for sorting of the protein to peroxisomes. Careful inspection of ultrathin sections of methanol-grown *H. polymorpha* wild-type cells labeled with anti-catalase antiserum revealed that the specific labeling was invariably confined to peroxisomes (Fig. 1A). The labeling is located at the periphery of the organelle at the space between the central alcohol oxidase crystalloid and the peroxisomal membrane, in line with earlier observations [30]. When the extreme C-terminal residue of catalase was mutated into K (Cat-SKK) labeling was observed in the cytosol, but not in peroxisomes, confirming that the C-terminal Ile residue is essential for targeting of the protein to peroxisomes (Fig. 1B). Moreover, these data indicate that *H. polymorpha* catalase does not contain a second, internal targeting signal. In addition, cells producing Cat-SKK were defective in growth on methanol (data not shown), in line with previous reports that proper sorting of catalase to peroxisomes is essential to allow growth of cells on methanol as sole carbon source [12].

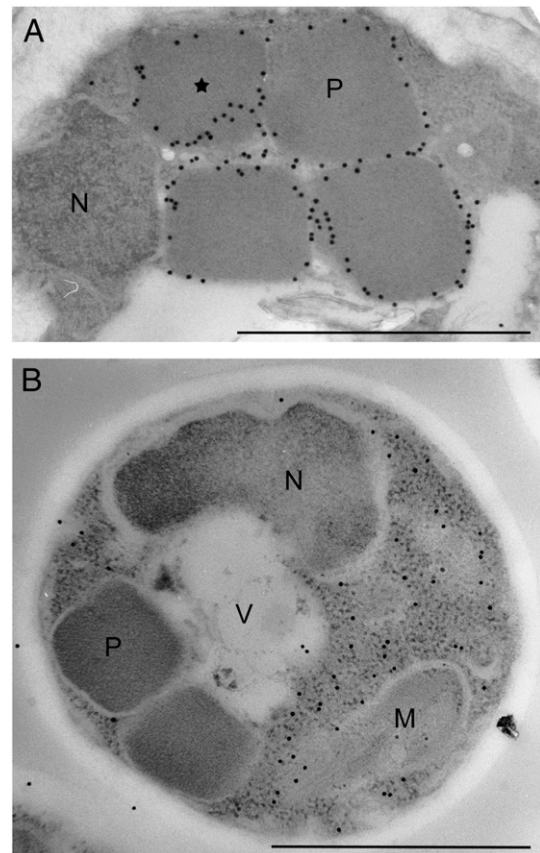


**Fig. 1.** The PTS1-SKI is essential for targeting catalase into peroxisomes of *H. polymorpha*. Immunocytochemical localization of catalase protein. In wild-type cells anti-catalase labeling is confined to the peroxisomal matrix (panel A), where labeling is observed between the alcohol oxidase crystalloid (asterisk) and the peroxisomal membrane. In the strain synthesizing Cat-SKK (panel B) catalase labeling is only observed in the cytosol. M—mitochondrion, N—nucleus, P—peroxisome, V—vacuole. The bar represents 1  $\mu$ m.

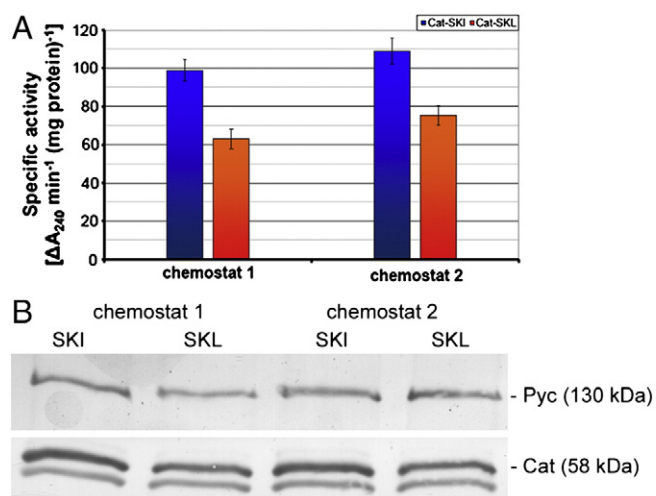


**Fig. 2.** Catalase enzyme activities are reduced in cells producing Cat-SKL. Cells of the Cat-SKI (blue) and Cat-SKL (red) strains were grown in methanol-limited chemostat cultures. Data are presented of two independent cultures at steady state. Panel A shows catalase enzyme activities in cell extracts of both cultures. The data show that cells of the Cat-SKL strain have a significantly lower catalase activity relative to the Cat-SKI strain. Panel B shows Western blots of the same cultures, decorated with anti-catalase antibodies. Below the catalase band is a non-specific band is present that also appears in a catalase deletion strain (data not shown). Equal amounts of protein were loaded per lane. Pyruvate carboxylase (Pyc) was used as loading control.

### 3.2. Changing the C-terminal -SKI of *H. polymorpha* catalase into -SKL results in a reduced growth yield during growth on methanol, accompanied by reduced catalase activities in vivo

To further analyze the importance of the non-canonical PTS1 of catalase, two identical strains were constructed in which the original catalase gene was replaced by a gene encoding either the wild-type protein (cat-SKI) or a mutated variant (cat-SKL). The strains were constructed in such a way that they were genetically identical (except for the codon encoding the last residue of the PTS1) and contained the catalase gene under control of their endogenous promoter.

In order to study the effect of the single amino acid substitution on cell physiology, both strains were grown in methanol-limited chemostat cultures. Peroxisomal catalase activity is essential to allow growth of cells on methanol at these conditions [31]. Hence,

minor deviations in enzyme activities or sorting are expected to affect the growth yields. The yield of the cultures (measured as optical densities at  $OD_{660}$ ) was determined in two independent, steady state cultures of both strains. These measurements revealed that at steady state conditions (over a period of more than 50 h) the  $OD_{660}$  of the Cat-SKL strain was significantly reduced ( $OD_{660} 4.22 \pm 0.04$ ) relative to that of the Cat-SKI strain ( $OD_{660} 4.69 \pm 0.20$ ).

Enzyme activity measurements in cell extracts of the two independent chemostat cultures of both strains revealed a significantly lower catalase activity in the Cat-SKL strain, namely a reduction of approx. ~35% (Fig. 2A). Western blot analysis indicated only a minor reduction in the levels of catalase protein in cells of the Cat-SKL strain relative to that of the cat-SKI strain (Fig. 2B). Densitometric scanning of the blots using the constitutive protein pyruvate carboxylase (Pyc) as loading control revealed that the catalase level was approx. 8% reduced in the cultures of the Cat-SKL strain. Hence, the reduction in enzyme activity can only partially be attributed to a reduction in catalase protein levels. As a consequence, a significant portion of the catalase protein in the Cat-SKL strain is apparently enzymatically inactive.

### 3.3. Cat-SKL cells contain catalase protein aggregates in peroxisomes

Immunolabeling experiments suggested that in Cat-SKI and Cat-SKL cells, all catalase protein was invariably localized to peroxisomes. These studies also showed however that electron dense protein aggregates occurred in the peroxisomal matrix of the Cat-SKL strain (Fig. 3A). These aggregates were never observed in peroxisomes of Cat-SKI cells (compare Fig. 1A). Immunolabeling revealed that these aggregates contained catalase protein (Fig. 3B). Together with the biochemical data presented in Section 3.2. these data suggest that a portion of the catalase-SKL is most likely present as inactive protein aggregates inside the organelles, possibly because the -SKL signal results in import of catalase protein that is not (yet) properly folded/assembled.

To test this, we constructed a mutant variant of catalase that is unable to fold properly. Heme binding is a pre requisite for catalase tetramerization [32] and disruptions to the heme binding pocket severely hinder catalase folding [33]. In the case of the catalase hydroperoxidase II (HPII) from *E. coli*, mutation of the proximal tyrosine residue completely abrogates heme binding, resulting in protein mis-folding [33]. The crystal structure of *H. polymorpha* catalase has recently been solved [15]. This study indicated that, as with other

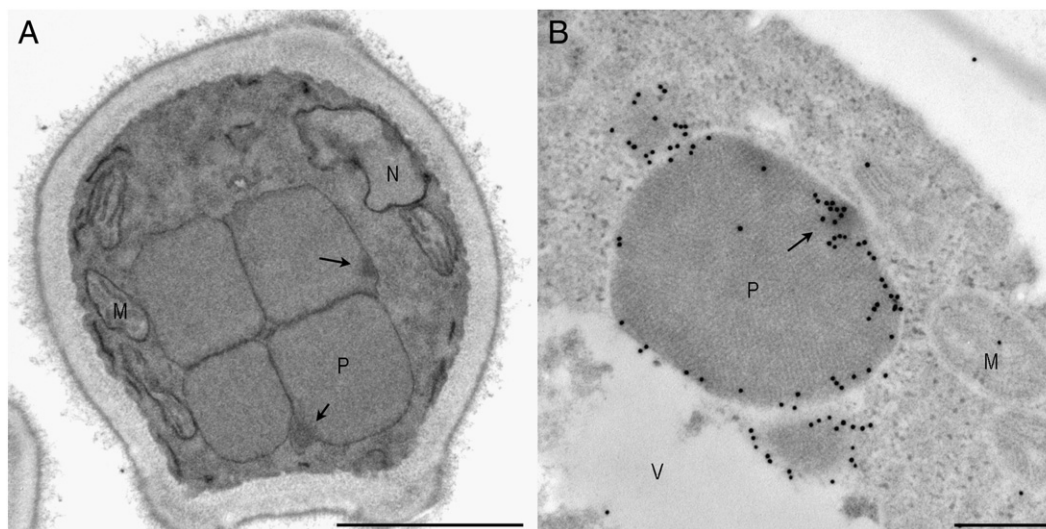


**Fig. 3.** Cells of the Cat-SKL strain contain catalase protein aggregates in the peroxisomal matrix. Immunolabeling of cells of the Cat-SKL strain showing the presence of electron dense protein aggregates in the peroxisomal matrix (panel A;  $\text{KMnO}_4$  fixation). Immunolabeling experiments using anti-catalase antibodies revealed that the electron dense aggregates contain catalase protein (panel B; aldehyde fixation). M—mitochondrion, N—nucleus, P—peroxisome, V—vacuole. The bar represents 1  $\mu\text{m}$  (A) or 0.2  $\mu\text{m}$  (B).

catalase structures, the heme binding pocket in *H. polymorpha* catalase is formed at the interface of two catalase subunits in the catalase tetramer, with tyrosine 348 acting as proximal, heme co-ordinating ligand. Hence, a gene was constructed, designed to hinder folding and tetramerization, that encodes a mutant form of *H. polymorpha* catalase, where tyrosine 348 was replaced with a glycine (Cat-Y348G). The mutant gene was expressed under control of the *H. polymorpha* catalase promoter in a strain in which the endogenous catalase gene was disrupted. As expected, the cells completely lacked catalase enzyme activity and were unable to grow on methanol (data not shown). Immunolabeling experiments using anti-catalase antiserum indicated that the bulk of the Cat-Y348G protein was present in electron dense aggregates in the cytosol and only a minor portion was present in peroxisomes (Fig. 4A). This observation suggests that the block in heme binding indeed severely affected catalase protein folding. The minor portion of the catalase protein inside peroxisomes could indicate however, that import of catalase protein can occur without heme binding or proper protein folding. To test whether more protein would be imported upon replacing the endogenous PTS1 by the stronger SKL sequence, we constructed a strain that produced a mutant variant with both the Cat-Y348G mutation together with the strong PTS1 sequence -SKL (Cat-Y348G-SKL). Immunolabeling experiments revealed that in this strain anti-catalase labeling was confined to peroxisomes, where the protein was observed as electron dense spots, representing catalase protein aggregates (Fig. 4B).

#### 3.4. *H. polymorpha* Pex5p exhibits an 8 fold lower binding to -SKI over -SKL

In order to determine the effect an Ile residue in the -1 position has on Pex5p binding, we designed peptides consisting of the last 12 amino acids of catalase (plus an extra Tyr residue at the N-terminus, to aid concentration determination), where the last residue was either Leu or Ile (YELKRRKASSPSKI/L) and performed ITC (Table 5). Interestingly, we observed that Pex5p exhibits an 8-fold lower binding affinity for the -SKI peptide relative to the -SKL form, indicating that -SKI is a less efficient targeting sequence in comparison to -SKL.

#### 3.5. SKI reduces the efficiency of import of the model protein GFP relative to -SKL

In order to test whether the reduced affinity of the -SKI signal for Pex5 relative to -SKL affects peroxisomal protein sorting, we compared import of the fluorescent protein GFP containing either the -SKI [34] or -SKL peroxisomal targeting sequence [35]. In both strains GFP is extended only by the tripeptides (i.e. without any linkers; [34,35]). GFP-SKL or GFP-SKI was produced in wild-type *H. polymorpha* cells under control of the inducible alcohol oxidase promoter ( $P_{AOX}$ ). The expression cassettes were integrated at the  $P_{AOX}$  locus [34,35]. During growth of cells on glucose the  $P_{AOX}$  is fully repressed, resulting in the absence of fluorescence in the cells (data not shown). However, upon a shift to inducing conditions (methanol media) expression is induced. As shown in Fig. 5, GFP fluorescence was observed in the cells of both strains that were induced for 4 h. In cells of the Cat-SKL strain fluorescence was confined to peroxisomes. By contrast, in cells producing GFP-SKI both cytosolic and peroxisomal fluorescence was observed (Fig. 5). This difference suggests that import of GFP-SKI is less efficient relative to GFP-SKL in vivo.

**Table 5**  
Summary of the ITC data.

Peptide	Kd ( $\mu$ M)	$\Delta H$ (Kcal mol <sup>-1</sup> )	$T\Delta S$ (Kcal mol <sup>-1</sup> )	$\Delta G$ (Kcal mol <sup>-1</sup> )	n
-SKI	21.9 ± 5.6	8.7 ± 2.2	15.0 ± 2.4	-6.4 ± 0.2	0.91 ± 0.01
-SKL	2.9 ± 0.4	7.4 ± 0.8	15.0 ± 0.9	-7.5 ± 0.1	0.95 ± 0.02

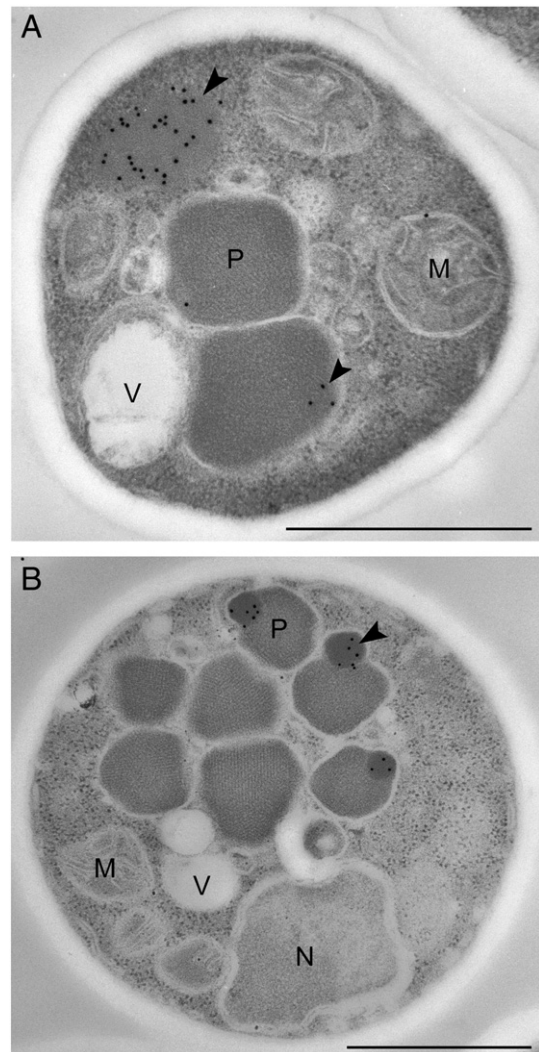


**Fig. 4.** Catalase containing a mutation in the heme binding site accumulates in the cytosol, but is present in the peroxisome when the PTS1 is changed into -SKL. Immunocytochemical staining of catalase protein in cells producing Cat-Y348G (panel A) or Cat-Y348G-SKL (panel B). The micrographs show that the protein containing the endogenous PTS (panel A) is predominantly present as electron dense aggregates in the cytosol, whereas a minor portion is present in an aggregate inside peroxisomes. The same mutant protein containing a C-terminal -SKL is only observed in aggregates in the peroxisomal matrix (panel B). M—mitochondrion, N—nucleus, P—peroxisome, V—vacuole. Arrows — protein aggregates. The bar represents 1  $\mu$ m.

Western blotting revealed that the levels of GFP as well as two key proteins involved in PTS1 protein import, Pex5 and Pex14, were similar in both strains (Fig. 5). Therefore, our data are consistent with the view that the observed differences in import efficiency are related to the reduced affinity of -SKI to Pex5p, relative to -SKL rather than a result of differences in GFP, Pex5p and Pex14p protein levels.

#### 3.6. Modeling of Pex5p binding to catalase SKI

A closer look at the eight Pex5p-cargo structures currently available provides an insight into the contrasting behavior of the SKI/SKL versions of catalase (Fig. 6). The actual C-terminal residue of the PTS1 does not make specific contacts with Pex5p. Instead, the carboxyl group of the poly-peptide backbone contacts a pair of Asn residues (Fig. 6) that are conserved in Pex5p from different species [36]. In all eight Pex5p-cargo structures, the PTS1 is in the same orientation with relation to Pex5p and although the PTS1 in each protein/peptide contains a Leu at the extreme C-terminus, the requirement of the conserved Asn residues for all Pex5p-PTS1 interactions [36] indicates

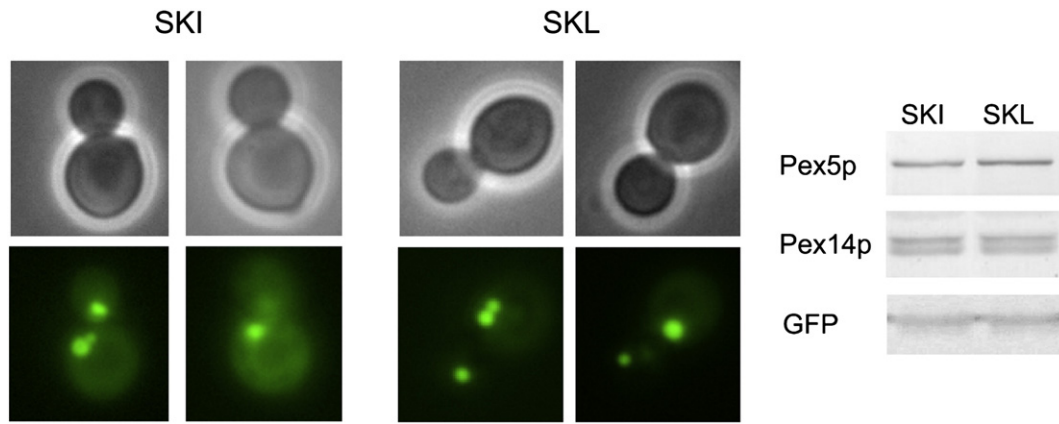


**Fig. 5.** GFP-SKI has a longer residence time in the cytosol relative to GFP-SKL. Cells producing GFP-SKL or GFP-SKI both under control of the inducible alcohol oxidase promoter were pre-cultivated on media containing glucose and then transferred to methanol containing media to induce the alcohol oxidase promoter. Fluorescence microscopy images were made 4 h after transferring the cells to methanol medium. In cells producing GFP-SKI cytosolic fluorescence is clearly present in addition to peroxisomal fluorescence. In cells of the GFP-SKL strain cytosolic fluorescence is much lower as compared to the GFP-SKI strain. Western blots were decorated with specific antibodies against Pex5p, Pex14p and GFP. The levels of these proteins were similar in both strains. Identical amounts of protein were loaded to each lane from cell lysates of cells induced for 4 h on methanol.

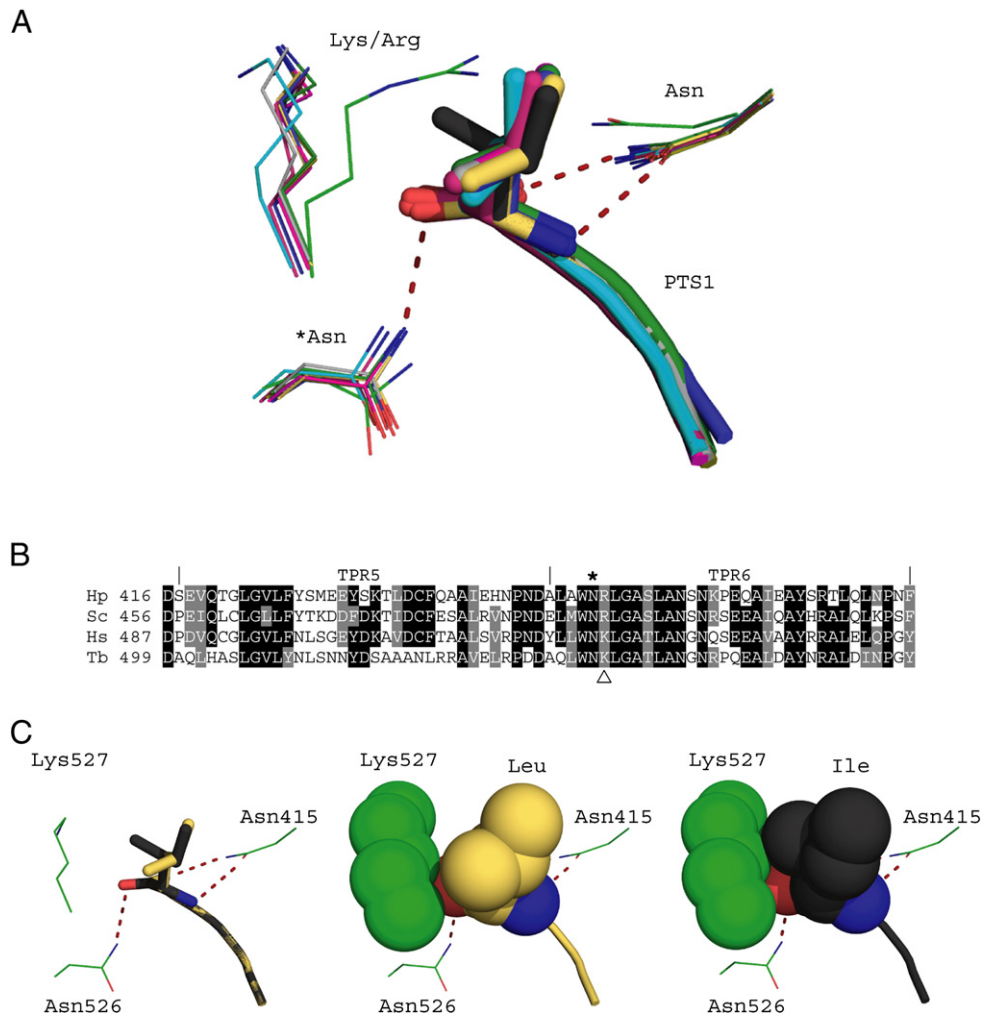


**Fig. 6.** Model of catalase-SKI binding to Pex5p. (Panel A) Structural superimposition of the eight Pex5p–cargo co-crystal structures (see text for details), as well as the *H. polymorpha* Pex5p (green) and -SKI PTS1 (black) models. The conserved lysine/arginine (Lys/Arg) residues in Pex5p that form the end of the PTS1 binding pockets are indicated, as are the conserved asparagine (Asn) residues that hydrogen bond to the poly-peptide backbone of the PTS1. (B) Sequence alignment of the fifth and sixth tetratricopeptide repeat (TPR) regions of *H. polymorpha* (Hp), *S. cerevisiae* (Sc), *H. sapiens* (Hs) and *T. brucei* (Tb) Pex5p, indicating the conserved asparagine (\*, also shown with asterisk in (A)) and lysine/arginine residue (open triangle). (C) Possible mode of binding of a PTS1 with Leu (yellow) or Ile (black) at –1 position to human Pex5p (PDB code 1FCH, green), showing the clash between the C $\beta$  methyl group of Ile and lysine 527 (right panel). (For interpretation of the references to color in this figure legend, the reader is referred to the web version of this article.)



that the orientation of the PTS1 is conserved. This allowed us to model how Pex5p may bind to a PTS1 with Ile in the  $-1$  position (Fig. 6). Ile and Leu are stereoisomers and chemically identical. The only difference comes in the position of a single methyl group, either branching from the C $\beta$  in Ile or from C $\gamma$  in Leu. We observed that the methyl group from Ile could clash with the residue that forms the end of the PTS1 binding pocket in both our model of *H. polymorpha* Pex5p as well as the human and trypanosome protein structures (Fig. 6). Such a clash would undoubtedly lead to a lower binding affinity for a PTS1 containing an Ile at position  $-1$ , when compared to one with Leu at the equivalent position. To test this hypothesis, we attempted to mutate this residue in HpPex5p, which is Arg 455, to an alanine, to create a larger PTS1 binding pocket. However, we were unable to purify this mutant protein from *E. coli*, as it was insoluble. In the structures, the equivalent residue participates in hydrogen binding with a number of other residues in the Pex5p core and mutating it very likely destabilizes the protein.

#### 4. Discussion

We showed that in the context of a 13-mer the C-terminal tripeptide of the PTS1 of *H. polymorpha* catalase (-SKI) has an eight fold lower affinity for its receptor Pex5 relative to the typical PTS1 tripeptide -SKL. Additionally, our model of how Pex5p may bind -SKI identifies a potential clash between the Ile at the  $-1$  position and residues in the PTS1 binding pocket, which would very likely inhibit the interaction and consequently result in a somewhat slower import of the catalase protein (Fig. 6). Indeed, our fluorescence microscopy studies using GFP-SKL and GFP-SKI revealed that GFP-SKI has a longer residence time in the cytosol relative to the GFP-SKL protein (Fig. 5).

Inspection of the C-terminal sequences of peroxisome borne catalases that were experimentally demonstrated to be located inside peroxisomes (Table 1) revealed that none of these enzymes contains a C-terminal -SKL. Moreover, most of these enzymes have a C-terminal tripeptide that does not correspond to the PTS1 consensus sequence. As a consequence, all peroxisomal catalases most likely have a relatively low affinity for their PTS1 receptors.

An intriguing question is why this crucial peroxisomal enzyme does not contain a strong PTS1, in order to ensure efficient sorting of the protein to peroxisomes under all circumstances. Our current data suggest that the strong -SKL sequence, but not the endogenous -SKI sequence, may result in import of catalase protein molecules that are not yet properly folded.

We show that a mutation in the heme binding site of catalase results in the formation of catalase-containing protein aggregates in the cytosol, providing a link between correct folding/oligomerisation and targeting. However, if the same mutated catalase variant contains the tripeptide -SKL, catalase protein aggregates are observed inside peroxisomes.

Based on these observations we speculate that in wild-type cells the weak -SKI sequence may prevent import of not yet folded catalase molecules. Indeed, we did not observe catalase aggregates in peroxisomes of wild-type cells that produce Cat-SKI. In contrast however, the strain that produces catalase protein with the stronger -SKL sequence (Cat-SKL) contained reduced catalase enzyme activity and had catalase aggregates inside peroxisomes. It is therefore tempting to speculate that the weak nature of the PTS1 in catalase acts as a quality control factor, allowing only correctly folded proteins to be imported.

Experiments using methanol-limited chemostat cultures revealed that the lower level of catalase enzyme activity of cells of the Cat-SKL strain has a physiological relevance, as the growth yield was reduced relative to that in cells of the Cat-SKI strain. This reduction is most likely due to the fact that in this strain H<sub>2</sub>O<sub>2</sub> is decomposed by

other, energy-requiring processes, e.g. via cytochrome c peroxidase [31].

The import and assembly pathway of catalase has been studied in detail in various organisms. Early pulse chase studies using rat liver suggested that monomeric catalase is imported into the peroxisome matrix, followed by heme-binding and tetramerization inside the organelle [37]. Also, data from a recent in vitro protein binding study using purified human Pex5 and catalase, suggested that catalase is imported as a monomer, because Pex5 did preferentially bind monomeric catalase under the experimental conditions used. These analyses however did not include protein transport assays and therefore the relevance of these observations for protein translocation is not yet known [38]. Moreover, import of monomeric catalase into peroxisome implies that its co-factor heme, which is generally assumed to be only synthesized in mitochondria, has to be imported into peroxisomes. So far, no evidence has been presented that supports transport of heme across the peroxisomal membrane or heme biosynthesis inside peroxisomes.

Yet available in vivo studies provide evidence in support of the fact that catalase is imported as the active, assembled tetrameric protein in human fibroblasts [39,40] and in the yeast *C. boidinii* [11]. Given the fact that so far no molecular chaperones have been identified inside yeast peroxisomes, it is likely that peroxisomal enzymes fold and assemble with the help of cytosolic chaperones in the cytosol prior to translocation across the peroxisomal membrane. In line with this assumption is the observation that the peroxisomal translocan can accommodate large, oligomeric proteins [41–43]. Indeed, we previously showed that in *H. polymorpha* folded, oligomeric enzymes, such as dimeric dihydroxyacetone synthase and catalase, can be imported into peroxisomes [44]. Again, the absence of molecular chaperones inside yeast peroxisomes also implies that unfolded proteins inside these organelles are most likely unable to refold. Our data suggest that a portion of the Cat-SKL protein may bind to the Pex5 receptor before folding/assembly and hence ends up in protein aggregates inside the organelles (Fig. 3). Our studies using the Cat-Y348G-SKL strain confirm that Pex5 is capable to import a misfolded cargo protein (Fig. 4B).

Based on our findings we speculate that wild-type catalase protein (Cat-SKI) has an extended residence time in the cytosol relative to Cat-SKL. This extended period may also allow proper folding and assembly including binding of the co-factor heme. Folding is most likely mediated by cytosolic chaperones prior to binding of the protein to Pex5, resulting in efficient import of enzymatically active catalase protein. The Cat-SKL protein is also properly imported into peroxisomes, however, a portion of this variant most likely already binds Pex5 before being assembled. This protein will end up as aggregates in the organellar matrix.

In contrast to peroxisomes in mammals and fungi, chaperones have been identified in plant peroxisomes [45–47]. As plant catalases also contain non-canonical PTS1 sequences (Table 1), we speculate that these proteins are also folded in the cytosol, prior to import. If so, the chaperones identified may function in refolding of matrix proteins that become unfolded after import into peroxisomes, e.g. upon heat stress.

In conclusion, our results lend support to the notion that reducing the import rate of *H. polymorpha* catalase serves an important function, as it will allow proper folding of the enzyme prior to import. Based on this it is therefore tempting to speculate that similar mechanisms may exist for other complex peroxisomal proteins.

#### Acknowledgements

We thank Bert Jan Baas, Ron Booij, Annemarie Kralt and Niclas Schiller for technical assistance in various parts of the work and Arjen Krikken for critically reading the manuscript. E. Bener Aksam and K. Gunkel were supported by the Netherlands Organisation for

Scientific Research (ALW/NWO). C. Williams was funded by a Rubicon Fellowship (825.08.023) from NWO. We thank the EMBL Hamburg for providing resources and the SPC facility (EMBL Hamburg) for technical support. This project was carried out within the research program of the Kluyver Centre for Genomics of Industrial Fermentation, which is part of the Netherlands Genomics Initiative and NWO.

## References

- [1] A. Deisseroth, A.L. Dounce, Catalase: physical and chemical properties, mechanism of catalysis, and physiological role, *Physiol. Rev.* 50 (1970) 319–375.
- [2] T. Gabaldon, Peroxisome diversity and evolution, *Philos. Trans. R. Soc. Lond. B Biol. Sci.* 365 (2010) 765–773.
- [3] M. Skoneczny, A. Chelstowska, J. Rytka, Study of the coinduction by fatty acids of catalase A and acyl-CoA oxidase in standard and mutant *Saccharomyces cerevisiae* strains, *FEBS J.* 174 (1988) 297–302.
- [4] E. Gonzalez, The C-terminal domain of plant catalases. Implications for a glyoxysomal targeting sequence, *FEBS J.* 199 (1991) 211–215.
- [5] R.T. Mullen, M.S. Lee, R.N. Trelease, Identification of the peroxisomal targeting signal for cottonseed catalase, *Plant J.* 12 (1997) 313–322.
- [6] G. Neuberger, S. Maurer-Stroh, B. Eisenhaber, A. Hartig, F. Eisenhaber, Motif refinement of the peroxisomal targeting signal 1 and evaluation of taxon-specific differences, *J. Mol. Biol.* 328 (2003) 567–579.
- [7] T. Lingner, A.R. Kataya, G.E. Antonicelli, A. Benichou, K. Nilssen, X.Y. Chen, T. Siemsen, B. Morgenstern, P. Meinicke, S. Reumann, Identification of novel plant peroxisomal targeting signals by a combination of machine learning methods and in vivo subcellular targeting analyses, *Plant Cell* 23 (2011) 1556–1572.
- [8] C. Brocard, A. Hartig, Peroxisome targeting signal 1: is it really a simple tripeptide? *Biochim. Biophys. Acta* 1763 (2006) 1565–1573.
- [9] Y. Elgersma, A. Vos, M. van den Berg, C.W. van Roermund, P. van der Sluijs, B. Distel, H.F. Tabak, Analysis of the carboxyl-terminal peroxisomal targeting signal 1 in a homologous context in *Saccharomyces cerevisiae*, *J. Biol. Chem.* 271 (1996) 26375–26382.
- [10] G. Lametschwandner, C. Brocard, M. Fransen, P. Van Veldhoven, J. Berger, A. Hartig, The difference in recognition of terminal tripeptides as peroxisomal targeting signal 1 between yeast and human is due to different affinities of their receptor Pex5p to the cognate signal and to residues adjacent to it, *J. Biol. Chem.* 273 (1998) 33635–33643.
- [11] H. Horiguchi, H. Yurimoto, T. Goh, T. Nakagawa, N. Kato, Y. Sakai, Peroxisomal catalase in the methylotrophic yeast *Candida boidinii*: transport efficiency and metabolic significance, *J. Bacteriol.* 183 (2001) 6372–6383.
- [12] T. Didion, R. Roggenkamp, Targeting signal of the peroxisomal catalase in the methylotrophic yeast *Hansenula polymorpha*, *FEBS Lett.* 303 (1992) 113–116.
- [13] P.E. Purdew, S.M. Castro, V. Protopopov, P.B. Lazarow, Targeting of human catalase to peroxisomes is dependent upon a novel C-terminal peroxisomal targeting sequence, *Ann. N. Y. Acad. Sci.* 804 (1996) 775–776.
- [14] F. Kragler, A. Langeder, J. Raupachova, M. Binder, A. Hartig, Two independent peroxisomal targeting signals in catalase A of *Saccharomyces cerevisiae*, *J. Cell Biol.* 120 (1993) 665–673.
- [15] E. Pena-Soler, M.C. Vega, M. Wilmanns, C. Williams, Structural features of peroxisomal catalase from the yeast *Hansenula polymorpha*, *Acta Crystallogr. D Biol. Crystallogr.* 67 (2011) 690–698.
- [16] M.J. Mate, M. Zamocky, L.M. Nykyri, C. Herzog, P.M. Alzari, C. Betzel, F. Koller, I. Fita, Structure of catalase-A from *Saccharomyces cerevisiae*, *J. Mol. Biol.* 286 (1999) 135–149.
- [17] A. Kamigaki, S. Mano, K. Terauchi, Y. Nishi, Y. Tachibe-Kinoshita, K. Nito, M. Kondo, M. Hayashi, M. Nishimura, M. Esaka, Identification of peroxisomal targeting signal of pumpkin catalase and the binding analysis with PTS1 receptor, *Plant J.* 33 (2003) 161–175.
- [18] G.J. Gatto Jr., E.L. Maynard, A.L. Guerrero, B.V. Geisbrecht, S.J. Gould, J.M. Berg, Correlating structure and affinity for PEX5:PTS1 complexes, *Biochemistry* 42 (2003) 1660–1666.
- [19] E.L. Maynard, G.J. Gatto Jr., J.M. Berg, Pex5p binding affinities for canonical and noncanonical PTS1 peptides, *Proteins* 55 (2004) 856–861.
- [20] D. Ghosh, J.M. Berg, A proteome-wide perspective on peroxisome targeting signal 1 (PTS1)–Pex5p affinities, *J. Am. Chem. Soc.* 132 (2010) 3973–3979.
- [21] J. Sambrook, E.F. Fritsch, T. Maniatis, *Molecular Cloning: A Laboratory Manual*, 2nd ed. Cold Spring Harbor Laboratory, New York, 1989.
- [22] I.J. van der Klei, W. Harder, M. Veenhuis, Selective inactivation of alcohol oxidase in two peroxisome-deficient mutants of the yeast *Hansenula polymorpha*, *Yeast* 7 (1991) 813–821.
- [23] H. Luck, *Methods of Enzymatic Analysis*, Academic Press, New York, 1963.
- [24] U.K. Laemmli, Cleavage of structural proteins during the assembly of the head of bacteriophage T4, *Nature* 227 (1970) 680–685.
- [25] J. Kyhse-Andersen, Electrophoresis of multiple gels: a simple apparatus without buffer tank for rapid transfer of proteins from polyacrylamide to nitrocellulose, *J. Biochem. Biophys. Methods* 10 (1984) 203–209.
- [26] H.R. Waterham, V.I. Titorenko, P. Haima, J.M. Cregg, W. Harder, M. Veenhuis, The *Hansenula polymorpha* PER1 gene is essential for peroxisome biogenesis and encodes a peroxisomal matrix protein with both carboxy- and amino-terminal targeting signals, *J. Cell Biol.* 127 (1994) 737–749.
- [27] W.A. Stanley, F.V. Filipp, P. Kursula, N. Schuller, R. Erdmann, W. Schliebs, M. Sattler, M. Wilmanns, Recognition of a functional peroxisome type 1 target by the dynamic import receptor pex5p, *Mol. Cell* 24 (2006) 653–663.
- [28] G.J. Gatto Jr., B.V. Geisbrecht, S.J. Gould, J.M. Berg, Peroxisomal targeting signal-1 recognition by the TPR domains of human PEX5, *Nat. Struct. Biol.* 7 (2000) 1091–1095.
- [29] P. Emsley, B. Lohkamp, W.G. Scott, K. Cowtan, Features and Development of Coot, *Acta Crystallogr. D Biol. Crystallogr.* 66 (2010) 486–501.
- [30] I. Keizer, R. Roggenkamp, W. Harder, M. Veenhuis, Location of catalase in crystalline peroxisomes of methanol-grown *Hansenula polymorpha*, *FEMS Microbiol. Lett.* 72 (1992) 7–11.
- [31] C. Verduyn, M.L. Giuseppin, W.A. Scheffers, J.P. van Dijken, Hydrogen peroxide metabolism in yeasts, *Appl. Environ. Microbiol.* 54 (1988) 2086–2090.
- [32] H. Ruis, The biosynthesis of catalase, *Can. J. Biochem.* 57 (1979) 1122–1130.
- [33] M.S. Sevinc, J. Switala, J. Bravo, I. Fita, P.C. Loewen, Truncation and heme pocket mutations reduce production of functional catalase HPII in *Escherichia coli*, *Protein Eng.* 11 (1998) 549–555.
- [34] F.A. Salomons, J.A. Kiel, K.N. Faber, M. Veenhuis, I.J. van der Klei, Overproduction of Pex5p stimulates import of alcohol oxidase and dihydroxyacetone synthase in a *Hansenula polymorpha* Pex14 null mutant, *J. Biol. Chem.* 275 (2000) 12603–12611.
- [35] A.N. Leao-Helder, A.M. Krikken, I.J. van der Klei, J.A. Kiel, M. Veenhuis, Transcriptional down-regulation of peroxisome numbers affects selective peroxisome degradation in *Hansenula polymorpha*, *J. Biol. Chem.* 278 (2003) 40749–40756.
- [36] A.T. Klein, P. Barnett, G. Bottger, D. Konings, H.F. Tabak, B. Distel, Recognition of peroxisomal targeting signal type 1 by the import receptor Pex5p, *J. Biol. Chem.* 276 (2001) 15034–15041.
- [37] P.B. Lazarow, C. de Duve, The synthesis and turnover of rat liver of rat liver peroxisomes. IV. Biochemical pathway of catalase synthesis, *J. Cell Biol.* 59 (1973) 491–506.
- [38] M.O. Freitas, T. Francisco, T.A. Rodrigues, I.S. Alencastre, M.P. Pinto, C.P. Grou, A.F. Carvalho, M. Fransen, C. Sa-Miranda, J.E. Azevedo, PEX5 protein binds monomeric catalase blocking its tetramerization and releases it upon binding the N-terminal domain of PEX14, *J. Biol. Chem.* 286 (2011) 40509–40519.
- [39] E. Middelkoop, E.A. Wiemer, D.E. Schoenmaker, A. Strijland, J.M. Tager, Topology of catalase assembly in human skin fibroblasts, *Biochim. Biophys. Acta* 1220 (1993) 15–20.
- [40] J.I. Koepke, K.A. Nakrieko, C.S. Wood, K.K. Boucher, L.J. Terlecky, P.A. Walton, S.R. Terlecky, Restoration of peroxisomal catalase import in a model of human cellular aging, *Traffic* 8 (2007) 1590–1600.
- [41] P.A. Walton, P.E. Hill, S. Subramani, Import of stably folded proteins into peroxisomes, *Mol. Biol. Cell* 6 (1995) 675–683.
- [42] S.J. Gould, C.S. Collins, Opinion: peroxisomal-protein import: is it really that complex? *Nat. Rev. Mol. Cell Biol.* 3 (2002) 382–389.
- [43] M. Meinecke, C. Cizmowski, W. Schliebs, V. Kruger, S. Beck, R. Wagner, R. Erdmann, The peroxisomal importomer constitutes a large and highly dynamic pore, *Nat. Cell Biol.* 12 (2011) 273–277.
- [44] K.N. Faber, R. van Dijk, I. Keizer-Gunnink, A. Koek, I.J. van der Klei, M. Veenhuis, Import of assembled PTS1 proteins into peroxisomes of the yeast *Hansenula polymorpha*: yes and no! *Biochim. Biophys. Acta* 1591 (2002) 157–162.
- [45] C. Carrie, E. Giraud, O. Duncan, L. Xu, Y. Wang, S. Huang, R. Clifton, M. Murcha, A. Filipovska, O. Rackham, A. Vrieland, J. Whelan, Conserved and novel functions for *Arabidopsis thaliana* MIA40 in assembly of proteins in mitochondria and peroxisomes, *J. Biol. Chem.* 285 (2010) 36138–36148.
- [46] C. Ma, M. Haslbeck, L. Babujee, O. Jahn, S. Reumann, Identification and characterization of a stress-inducible and a constitutive small heat-shock protein targeted to the matrix of plant peroxisomes, *Plant Physiol.* 141 (2006) 47–60.
- [47] B. Wimmer, F. Lottspeich, I. van der Klei, M. Veenhuis, C. Gietl, The glyoxysomal and plastid molecular chaperones (70-kDa heat shock protein) of watermelon cotyledons are encoded by a single gene, *Proc. Natl. Acad. Sci. U. S. A.* 94 (1997) 13624–13629.
- [48] M. Esaka, N. Yamada, M. Kitabayashi, Y. Setoguchi, R. Tsugeki, M. Kondo, M. Nishimura, cDNA cloning and differential gene expression of three catalases in pumpkin, *Plant Mol. Biol.* 33 (1997) 141–155.
- [49] L. Kawasaki, J. Aguirre, Multiple catalase genes are differentially regulated in *Aspergillus nidulans*, *J. Bacteriol.* 183 (2001) 1434–1440.
- [50] S.H. Togo, M. Maebuchi, S. Yokota, M. Bun-Ya, A. Kawahara, T. Kamiryo, Immunological detection of alkaline-diaminobenzidine-negative peroxisomes of the nematode *Caenorhabditis elegans* purification and unique pH optima of peroxisomal catalase, *FEBS J.* 267 (2000) 1307–1312.
- [51] R.N. Trelease, W. Xie, M.S. Lee, R.T. Mullen, Rat liver catalase is sorted to peroxisomes by its C-terminal tripeptide Ala-Asn-Leu, not by the internal Ser-Lys-Leu motif, *Eur. J. Cell Biol.* 71 (1996) 248–258.
- [52] N. Usuda, J.K. Reddy, T. Hashimoto, M.S. Rao, Immunocytochemical localization of liver-specific proteins in pancreatic hepatocytes of rat, *Eur. J. Cell Biol.* 46 (1988) 299–306.
- [53] S.P. Gleeson, MAG, genetic analysis in the methylotrophic yeast *Hansenula polymorpha*, *Yeast* 4 (1988) 293–303.
- [54] R. van Dijk, K.N. Faber, A.T. Hammond, B.S. Glick, M. Veenhuis, J.A. Kiel, Tagging *Hansenula polymorpha* genes by random integration of linear DNA fragments (RALF), *Mol. Genet. Genomics* 266 (2001) 646–656.
- [55] S.H. Klompmaker, A. Kilic, R.J. Baerends, M. Veenhuis, I.J. van der Klei, Activation of a peroxisomal *Pichia pastoris* D-amino acid oxidase, which uses d-alanine as a preferred substrate, depends on pyruvate carboxylase, *FEMS Yeast Res.* 10 (2010) 708–716.